



**HAL**  
open science

# Synthesis and Solid-State Properties of PolyC3 (Co)polymers Containing (CH<sub>2</sub>-CH<sub>2</sub>-C(COOR)<sub>2</sub>) Repeat Units with Densely Packed Fluorocarbon Lateral Chains

Nicolas Illy, Deogratias Urayeneza, Alina V. Maryasevskaya,, Laurent Michely,  
Sylvie Boileau, Blandine Brissault, Egor A. Bersenev, Denis V. Anokhin,  
Dimitri Ivanov, Jacques Penelle

► **To cite this version:**

Nicolas Illy, Deogratias Urayeneza, Alina V. Maryasevskaya,, Laurent Michely, Sylvie Boileau, et al.. Synthesis and Solid-State Properties of PolyC3 (Co)polymers Containing (CH<sub>2</sub>-CH<sub>2</sub>-C(COOR)<sub>2</sub>) Repeat Units with Densely Packed Fluorocarbon Lateral Chains. *Macromolecules*, 2019, 52 (23), pp.9199-9207. 10.1021/acs.macromol.9b01559 . hal-02370804

**HAL Id: hal-02370804**

**<https://hal.science/hal-02370804>**

Submitted on 7 Dec 2020

**HAL** is a multi-disciplinary open access archive for the deposit and dissemination of scientific research documents, whether they are published or not. The documents may come from teaching and research institutions in France or abroad, or from public or private research centers.

L'archive ouverte pluridisciplinaire **HAL**, est destinée au dépôt et à la diffusion de documents scientifiques de niveau recherche, publiés ou non, émanant des établissements d'enseignement et de recherche français ou étrangers, des laboratoires publics ou privés.

## CAUTION

This manuscript has been accepted after peer review and corresponds to a version prior to editing, proofreading, and formal publication. The final version available on the editor website may be different from this version as a result of the above editing process. Readers should consider obtaining the final version from the journal website if they want to ensure full accuracy of information. The corresponding authors can also be contacted in case of need.

# Synthesis and Solid-State Properties of PolyC<sub>3</sub> (Co)polymers Containing (CH<sub>2</sub>-CH<sub>2</sub>-C(COOR)<sub>2</sub>) Repeat Units With Densely Packed Fluorocarbon Lateral Chains

Nicolas Illy,<sup>◇,△</sup> Deogratias Urayeneza,<sup>◇</sup> Alina V. Maryasevskaya,<sup>§,‡,†</sup> Laurent Michely,<sup>◇</sup> Sylvie Boileau,<sup>◇</sup> Blandine Brissault,<sup>◇</sup> Egor A. Bersenev,<sup>‡,†</sup> Denis V. Anokhin,<sup>§,‡,†</sup> Dimitri A. Ivanov,<sup>\*,‡,||</sup>  
and Jacques Penelle<sup>\*,◇</sup>

<sup>◇</sup>Institut de Chimie et des Matériaux Paris-Est (East Paris Institute for Chemistry & Materials Science), Université Paris-Est and CNRS, 2-8 rue H. Dunant, F-94320 Thiais, France

<sup>△</sup>Sorbonne Université, CNRS, Institut Parisien de Chimie Moléculaire, Equipe Chimie des Polymères, 4 place Jussieu, F-75005 Paris, France

<sup>§</sup>Lomonosov Moscow State University (National Research University), Faculty of Fundamental Physical and Chemical Engineering, GSP-1, 1-51 Leninskie Gory, Moscow, Russian Federation

<sup>‡</sup>Moscow Institute of Physics and Technology (National Research University), Institutskiy per. 9, Dolgoprudny, Russian Federation

<sup>†</sup>Institute of Problems of Chemical Physics, Russian Academy of Sciences, Semenov Av. 1, Chernogolovka, Moscow Region, 142432, Russian Federation

<sup>||</sup>Institut de Sciences des Matériaux de Mulhouse-IS2M, CNRS UMR 7361, Jean Starcky, 15, F-68057 Mulhouse, France

**KEYWORDS:** Fluorinated polymers, semicrystalline and liquid crystalline polymers, structure-property relationships in the solid-state, self-associating side-chains in polymers, polymer synthesis, X-ray diffraction

**ABSTRACT:** The synthesis and structural characterization of linear PolyC<sub>3</sub> polymers containing trimethylene-1,1-dicarboxylate structural repeat units, with C<sub>6</sub>F<sub>13</sub> and C<sub>8</sub>F<sub>17</sub> fluorinated side chains is described for the first time, and their properties compared with the traditional polyvinyl structures that display the fluorinated chain on every second rather than on every third carbon alongside the backbone. Homopolymers as well as statistical and block copolymers with n-propyl and/or allyl trimethylene-1,1-dicarboxylate blocks have been obtained from PolyC<sub>3</sub> precursors containing diallyl trimethylene-1,1-dicarboxylate units, by reacting C<sub>6</sub>F<sub>13</sub>-C<sub>2</sub>H<sub>4</sub>-SH and C<sub>8</sub>F<sub>17</sub>-C<sub>2</sub>H<sub>4</sub>-SH thiols with the allyl groups using a thiol-ene post-polymerization modification reaction. Solid-state properties have been investigated by DSC for all the (co)polymers and by SAXS/WAXS for the C<sub>8</sub>F<sub>17</sub> homopolymer at several temperatures. The structure of the homopolymer consistently shows a coexistence of two smectic phases at room temperature, which can be identified as SmB and SmC. This coexistence is assumed to arise from the fact that the distances between carboxylic oxygens bonded to the same carbon are very close to the ones between the neighboring carboxylic oxygens alongside the backbone, resulting in two possible ways of packing the pendant fluoroalkyl chains arranged in an hexatic order.

## INTRODUCTION

Fluorinated macromolecules hold a distinctive place among organic polymers currently available to scientists and engineers. For instance, the chemical resistance of their C-F bonds, both to thermal and oxidative degradations, extends considerably the range of temperatures commercial polymers can be used routinely under aerobic atmospheres, polytetrafluoroethylene (PTFE, Teflon®) being the prototypical commercial example since 1946.<sup>1</sup> In addition, the presence of fluorinated chains made of  $(CF_2)_i$  and  $-CF_3$  units at the air- or liquid-polymer surface imparts low surface energies, hydro- and lipophobicities, as well as low adhesions and low surface frictions.<sup>1-2</sup> Finally, self-organization of the fluorinated chains close to the surface or in the bulk of the materials leads to thermal transitions arising from the semi-crystalline nature of the materials (PTFE in particular displays a very high propensity to crystallize) or from local lamellar arrangements. The structure and dynamics of these crystalline and liquid crystalline structures in turn impact surface (see above) and bulk properties such as solubility or gas transport.<sup>3</sup>

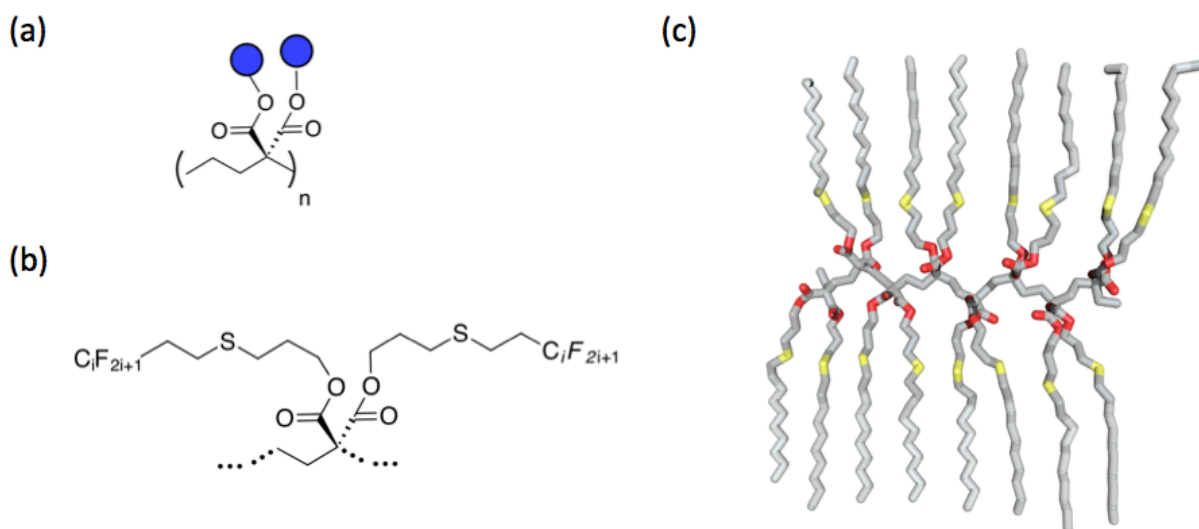
Although specific properties of partly fluorinated polymers can lead to other interesting applications (for example, as contrast agents in biomedical imaging or as permselective gas membranes),<sup>3,4</sup> the bulk of research efforts aimed at designing novel fluorinated polymers has been driven by the unique combination of their thermal/oxidative stability and surface properties. Over the years, many structures have been tested that can be schematically divided into two classes according to the positions where the fluorinated carbons can be found, i.e., in the main chain as in tetrafluoroethylene copolymers, or in side chains such as in polyacrylates presenting short or long perfluorinated carbon chains in the pendent esters. Combination of both structural arrangements can also be found, such as in commercial Nafion® polymers.

Thermal transitions – and to a certain point, surface properties as well – depend on the length of the  $(CF_2)_i$  units, but also on the aptitude of these fluorinated chains to straightforwardly self-organize into lamellae-type morphologies, with the fluorocarbon segments aligned in parallel. For side-chain systems, this ability will also depend upon the nature of the main chain on which the lateral segments are attached. More efficient arrangements will be attained when conformational minima for the main chain are easily accessible that favor the interactions between as many side chains as possible.

From that viewpoint, it would be interesting to systematically determine how the nature of the main chain, in particular the distance between branch points on the main chain alter the self-organization of lateral fluorinated chains and ultimately affect relevant bulk and surface properties. Indeed, most of the available literature on side-chain systems refer to poly(meth)acrylate polymers where the side chains are attached via an ester group on every second carbon alongside the main chain. A very recent contribution by the Ihara group looked at carbon-chain polymers substituted on every single carbon by ester bearing fluorinated side chains, providing evidences not only that these extremely crowded polymers were accessible but also that they exhibit solubility behavior in sharp contrast to polymers exhibiting the same fluorinated side-chain but on every second carbon.<sup>5</sup>

In this contribution, we wish to explore another substitution pattern in which two fluorinated side chains are attached on every third carbon on an all carbon-chain backbone (see Scheme 1a). In practice, this PolyC<sub>3</sub> geometry – in opposition to classical PolyC<sub>2</sub> geometries provided for example by polyacrylates, or to the PolyC<sub>1</sub> geometry mentioned in the previous paragraph – will be investigated via homo- and copolymers containing the structural repeat unit schematically provided in Scheme 1b. This arrangement provides a side-chain positioning that allows lateral

units to spread out efficiently and prevent steric crowding, while maintaining a very high degree of substitution along the backbone (Scheme 1c).



**Scheme 1.** (a) General structure of the PolyC<sub>3</sub> fluorinated polymers targeted in this study (the blue spheres indicate where the fluorinated side-chains will be placed); (b) actual structure of the repeat units incorporated in the investigated homo- and statistical copolymers (c) schematic rendering of an octameric fragment of a  $(\text{CH}_2\text{-CH}_2\text{-C}(\text{COO-X-R}_f)_2)_n$  polymer with a  $(\text{CH}_2)_3\text{S}(\text{CH}_2)_2$  X linker connecting the esters to the  $(\text{CF}_2)_7\text{CF}_3$  R<sub>f</sub> side chains (hydrogen and fluorine atoms have been omitted for the sake of clarity).

## EXPERIMENTAL SECTION

**Materials.** Monomer **1** (diallyl cyclopropane-1,1-dicarboxylate) and **2** (di-*n*-propyl cyclopropane-1,1-dicarboxylate) were synthesized according to previously described methods.<sup>6</sup> 1,4-Dioxane (99%, Carlo Erba), THF (99%, stabilized with BHT, Carlo Erba), chloroform (99%, VWR), acetone (99%, Aldrich), DMF (99%, Aldrich), DMSO (99.5%, VWR), ethanol (96%, Aldrich), methanol (technical grade, Aldrich), isopropanol (pure, Aldrich), phosphazene base

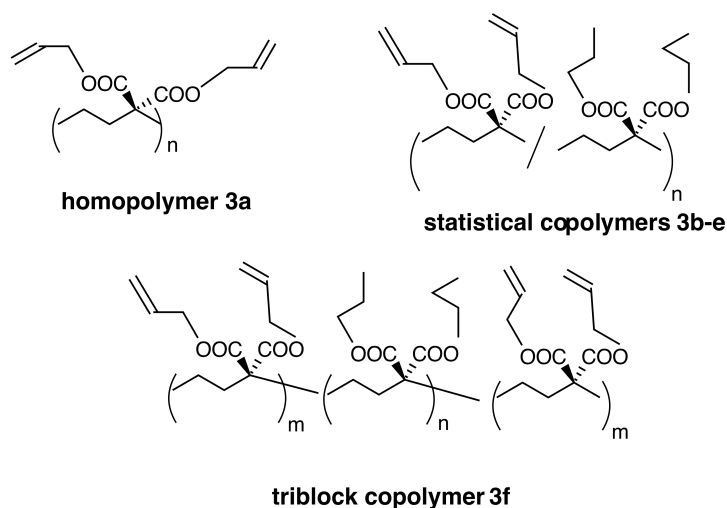
*t*BuP<sub>4</sub> solution (1.0 mol.L<sup>-1</sup> in hexane, Aldrich), thiophenol (≥ 99%, Aldrich), hydrochloric acid (35%, VWR Prolabo), and propan-1-ol (> 99%, Prolabo) were used as received. 2,2'-Azobis(isobutyronitrile) was recrystallized from diethyl ether and stored in the refrigerator. 3,3,4,4,5,5,6,6,7,7,8,8,9,9,10,10,10-heptafluorodecane-1-thiol [34143-74-3] and 3,3,4,4,5,5,6,6,7,7,8,8,8-tridecafluorooctane-1-thiol [34451-26-8] had been generously provided by Atochem (France) and were used as received. The THF used for anionic polymerizations was dried under benzophenone-Na.

**Polymeric Precursor 3a-f Synthesis.** Homo- and copolymers **3a-f** were obtained according to procedures described in a previous publication.<sup>6</sup> A general method for these polymerization is as follows:

Filling of the polymerization tube with the reagents prior to its closure was carried out in a glove-box. Monomer **1** (1.0 g, 4.76 mmol) is first introduced under argon into a polymerization tube fitted with a Rotaflo<sup>®</sup>. THF (1.00 mL), the required amounts of thiophenol and of phosphazene base solution in hexane (1.2 equivalent with respect to the thiol) are then successively added at room temperature using a microsyringe (the molar amount of PhSH depends upon the targeted degree of polymerization  $x_n$  according to equation  $x_n = [1]_0 / [PhSH]_0$ ). After careful closure of the reaction tube, the mixture is stirred at a set temperature for the minimal period of time required to obtain full conversion (the actual numbers depend upon the kinetics and can be found in the literature<sup>6</sup>). The reaction is then quenched with a large excess of a 12 mol.L<sup>-1</sup> HCl aqueous solution (20 equivalents with respect to the initiator precursor). The homopolymer **3a** is recovered by dissolution of the final mixture in chloroform and precipitation in methanol. The white powder obtained after filtration is dried under vacuum at 50°C for 48 h.

Statistical copolymers **3b-e** were obtained by copolymerizing mixtures of monomers **1** and **2**. The ABA block copolymer **3f** was synthesized by first polymerizing **2** using the bifunctional thiol bis(2-mercaptoethyl) ether as an initiator, and adding **1** in a second step after the full consumption of **2**.

Structures and molecular characteristics for all precursors are depicted in Scheme 2 and summarized in Table 1.



**Scheme 2.** Structures of the synthesized allyl-containing PolyC<sub>3</sub> (co)polymer precursors.

**Table 1.** Molecular weights and molar fraction of the precursor polymers **3a-f** (see Scheme 2).

	Polymer Architecture	M <sub>n</sub> (× 10 <sup>-3</sup> )		M <sub>w</sub> /M <sub>n</sub> SEC	Fraction of <b>1</b> (mol-%)
		SEC <sup>a</sup>	<sup>1</sup> H NMR <sup>b</sup>		
<b>3a</b>	homopolymer	9.2	10.0	1.21	100
<b>3b</b>	statistical copolymer	12.0	14.9 <sup>c</sup>	1.17	20
<b>3c</b>	statistical copolymer	11.0	15.7 <sup>c</sup>	1.23	40
<b>3d</b>	statistical	4.0	-	1.09	60

	copolymer				
<b>3e</b>	statistical copolymer	4.6	-	1.13	80
<b>3f</b>	triblock copolymer	9.3	11.5	1.10	60

<sup>a</sup> SEC-MALLS, <sup>b</sup> determined by comparing the signal ratios of protons on the PhS- end-group and on the backbone methylenes, respectively, and multiplying by the molecular weight of the repeat unit; <sup>c</sup> a larger than usual statistical experimental error was observed due to difficulties in adjusting the NMR phase for these samples.

**Fluorinated Polymer 4 Synthesis.** A solution containing 0.250 g of homopolymer **3a** (2.38 mmol of double bonds), 11.41 g of fluorinated thiol  $n\text{-C}_8\text{F}_{17}\text{-CH}_2\text{-CH}_2\text{-SH}$  (23.8 mmol, 10 eq.) and 0.195 g of AIBN (1.19 mmol, 0.5 eq.) in toluene (5.6 mL) was stirred under nitrogen until a full dissolution of all reagents was observed. The obtained homogeneous reaction mixture was then heated for 24 h at 80°C. Some cloudiness appeared in the solution over time. The solution was brought back to room temperature and added slowly to cold methanol. The obtained white solid was recovered by centrifugation (15 min at 4,000 rpm), and dried overnight under vacuum. Isolated yield: 1.286 g (92%).

**Fluorinated Polymer 5-10 Synthesis.** The above general procedure for polymer **4** was systematically carried out, using the following ratios for the reagents and solvent as calculated from the molar amount of available allyl branches on the reacted polymer: fluorinated thiol (10 eq.), AIBN (0.5 eq.), and toluene (8.0 mL.mol<sup>-1</sup> of C=C bonds).

**Instrumentation.** FTIR spectra were recorded on a TENSOR 27 Bruker spectrometer equipped with an ATR Digi Tect DLATGS detector (32 scans, 4 cm<sup>-1</sup> resolution) in the 500-4,000 cm<sup>-1</sup> range. <sup>1</sup>H and <sup>13</sup>C NMR spectra in solution were recorded on a Bruker Avance II

spectrometer operating at resonance frequencies of 400 and 100 MHz, respectively, using CDCl<sub>3</sub> as the solvent. The CP/MAS <sup>13</sup>C experiment on polymer **4** was carried out on a 400MHz Bruker spectrometer controlled by an Advance III console and equipped with a CP-MAS 4-mm low-gamma probe at a temperature of 293 K. The rotation speed was set at 6 kHz, relaxation delay D<sub>1</sub> at 5 s, PL<sub>1</sub> at 3.60 dB, contact time HP<sub>1</sub> at 3.25 μs and H-C exchange time p15 at 2385 μs. Chemical shift referencing was performed using adamantane.<sup>7</sup>

Size Exclusion Chromatography (SEC) experiments were performed in chloroform or THF (1.0 mL.min<sup>-1</sup>) at room temperature, using a Spectra Physics P100 pump, and two PLgel Polymer Laboratories linear columns (5 μm Mix-C, separation range: 200 to 2 x 10<sup>6</sup>). A Wyatt Technology Optilab Rex interferometric refractometer (690 nm laser) and a Wyatt Technology Minidawn light scattering photometer (three-angle detection, 20 mW semiconductor laser (690 nm)) were used as detectors.

DSC (Differential Scanning Calorimetry) measurements were carried out using a DSC Q100 model (TA Instruments) and a Diamond DSC (Perkin-Elmer) calibrated with indium standards. Samples were placed in an aluminum pan, and initially cooled at -50°C. Except when specifically mentioned, two heating (10 K.min<sup>-1</sup>) – cooling (40 K.min<sup>-1</sup>) cycles were then applied in the -50 – 150°C temperature range. Thermogravimetric experiments are based on the use of a LabSys evo TGA thermobalance (SETARAM Instrumentation, France).

Variable-temperature Small-Angle X-ray Scattering (SAXS) measurements were performed at the BM26B beamline of the European Synchrotron Radiation Facility (ESRF, Grenoble). The measurements were carried out in transmission using X-ray photons with the energy of 11.9 keV. Calibration of the norm of the reciprocal vector  $\mathbf{q}$  ( $|\mathbf{q}| = \frac{4\pi\sin(\theta)}{\lambda}$  where  $\theta$  is the Bragg angle and  $\lambda$ - wavelength) has been made using several diffraction orders of silver behenate.

Grazing-Incidence Wide-Angle X-ray Scattering (GIWAXS) measurements were performed using a laboratory SAXS/WAXS machine XeuSS (Xenocs, France) coupled to a GeniX3D generator ( $\lambda=1.54 \text{ \AA}$ ). The 2D data were collected at an incidence angle of  $0.18^\circ$  using a Rayonix HS170 CCD detector (pixel size  $132 \times 132 \mu\text{m}$ ) with sample to detector distance of approximately 18 cm. The minimum projection method applied to a series of images was used to subtract the background noise.

**Simulation.** Liquid crystalline (LC) structures were built and refined using the Forcite Geometry Optimization module of the Materials Studio package (Dassault Systems). To simulate the LC phase, an  $8 \times 8 \times 4$  non-periodic superstructure was used for the energy minimization with the COMPASS force field.

## RESULTS AND DISCUSSION

### Synthesis of Fluorinated Polymer 4.

The thiol-ene reaction of various thiols with non-activated C=C double bonds is usually an efficient approach when quantitative modification of a C=C-containing polymer is required.<sup>8</sup> Such a strategy has already been identified as suitable for the quantitative modification of PolyC<sub>3</sub> polymer **3a** or other PolyC<sub>3</sub> copolymers containing the same diallyl ester subunit as the one found in homopolymer **3a**.<sup>6</sup> Both photochemically and thermally AIBN-initiated reactions provided excellent results with mercaptans such as simple alkyl thiols, mercaptoalcohols or mercaptoaliphatic acids. The reaction has been extended further in order to laterally attach on a PolyC<sub>3</sub> backbone sugar thiols (to obtain glycopolymers designed for lectin specific recognition),<sup>9</sup> or lanthanide-chelating units (to obtain polymer monoclonal antibodies-conjugates for multiplexed immunoassays based on mass cytometry).<sup>10</sup>



trifluoromethylbenzene and 1,3-bis(trifluoromethyl)benzene (BTFB). In the later solvent, full solubility could be observed at high temperatures: for example, a 5 wt-% solution of **4** in BTFB was entirely homogeneous and transparent at 80-90°C, while precipitation occurred in the 50-60°C range when slowly lowering the temperature. Qualitatively comparing the above solubility data with other polymers described in the literature having a similar fluorinated lateral chain suggests that **4** is noticeably less soluble. Polyacrylates of different types,<sup>11-13</sup> poly(vinyl ether)s,<sup>14-15</sup> poly(2-oxazoline)s,<sup>16</sup> and poly(para-substituted tetrafluorostyrene),<sup>16</sup> all exhibit solubility at room temperature in organic solvents such as chloroform and, in the few cases they don't (mostly in the acrylate series), are soluble in fluorinated solvents. One exception to the above rule might be the substituted polymethylene (PolyC<sub>1</sub>) discussed in the Introduction although its solubility in fluorinated solvents has not been reported yet.<sup>5</sup>

A possible partial explanation for this observation might be related to the fact that **4** has two lateral fluorinated chains on a small repeat unit, thus generating a highly fluorine-rich polymers (e.g., the added thiol chains makes 82 wt-% of the total mass in **4** while the original **3a** backbone contributes only to the remaining 18 wt-%). In addition, the location of the ester groups on the polymer chain, with two lateral chains protruding from the backbone on every third carbon alongside the backbone (see Scheme 1c), generates a very high density of fluorinated grafts, which might “hide” the central chain and reinforce the polytetrafluoroethylene-like character of the polymer, including its low solubility.

The structure of **4** was fully confirmed by solid-state CP/MAS <sup>13</sup>C NMR and FT-IR (Figure 1). The NMR spectrum in particular includes all the expected signals for the assumed structure: the CF<sub>3</sub> and CF<sub>2</sub> peaks in the 105-125 ppm range,<sup>18-19</sup> the carbonyls at 170 ppm, the backbone CH<sub>2</sub> and quaternary C around 26 and 58 ppm, respectively, and the lateral methylene carbon directly

attached to the ester ( $-\text{C}(=\text{O})\text{O}-\underline{\text{C}}\text{H}_2-$ ) at 65 ppm.<sup>6</sup> The unaccounted carbons at this point (underlined in the linear formula available at the end of this sentence) all belong to the  $-\text{COO}-\underline{\text{C}}\text{H}_2-\underline{\text{C}}\text{H}_2-\underline{\text{C}}\text{H}_2-\text{S}-\underline{\text{C}}\text{H}_2-\underline{\text{C}}\text{H}_2-\text{CF}_2-$  lateral groups. NMR  $^{13}\text{C}$  chemical shift simulations based on group additivity theories indicate that all four remaining carbons for the above segment must be included in the broad intense signal appearing from 15 to 40 ppm, with theoretical chemical shifts expected at 34.3 ( $\text{S}-\underline{\text{C}}\text{H}_2-\underline{\text{C}}\text{H}_2-\text{CF}_2$ ), 29.7 ( $\text{COO}-\underline{\text{C}}\text{H}_2-\underline{\text{C}}\text{H}_2-\underline{\text{C}}\text{H}_2$ ), 28.3 ( $\text{COO}-\text{C}\text{H}_2-\text{C}\text{H}_2-\underline{\text{C}}\text{H}_2$ ) and 17.2 ppm ( $\text{S}-\underline{\text{C}}\text{H}_2-\text{C}\text{H}_2-\text{CF}_2$ ).<sup>20-21</sup> Despite their high concentration (14 carbons per structural repeat unit) and as expected based on the known literature,<sup>19</sup> the  $\text{CF}_2$  groups do not lead to very intense signals when compared to the other carbons, due to multiple couplings with  $^{19}\text{F}$  atoms and the influence of carbon perfluorination on  $^{13}\text{C}$  relaxations. Particularly significant with respect to the efficiency of the thiol-ene reaction is the absence of signals potentially arising from unreacted allyl units.<sup>6</sup> Both allyl signals expected at 66 ppm ( $-\text{COO}-\underline{\text{C}}\text{H}_2-\text{CH}=\text{CH}_2$ ) and 119 ppm ( $-\text{COO}-\text{C}\text{H}_2-\text{CH}=\underline{\text{C}}\text{H}_2$ ) are unfortunately partly hidden by other peaks, yet the strong signal expected for the  $-\text{COO}-\text{C}\text{H}_2-\underline{\text{C}}\text{H}=\text{CH}_2$  carbon should arise at 132 ppm where only a complete absence of signal can be found.

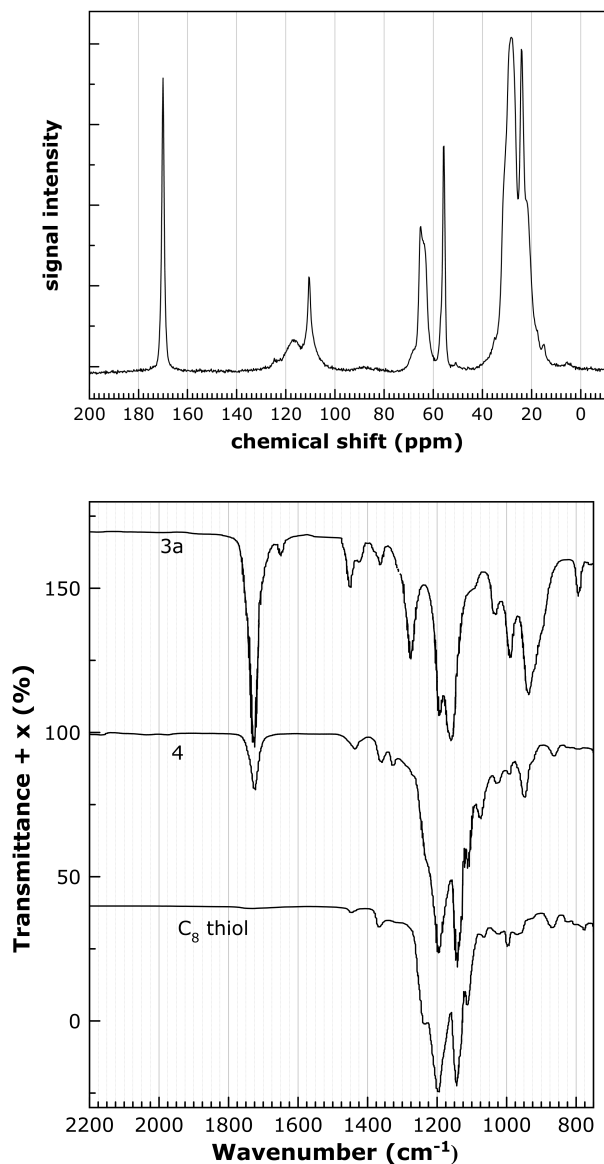


**Figure 1.** (Top) Solid-state (CP/MAS)  $^{13}\text{C}$  NMR spectrum of **4**; (bottom) overlaid IR spectra of starting polymer **3a**, modified polymer **4** and modifying agent  $\text{C}_8\text{F}_{17}\text{C}_2\text{H}_4\text{SH}$  (from top to bottom). The missing part of the spectra in the 2200-4000  $\text{cm}^{-1}$  region is available in Figure S1 in the Supplementary Materials document. The shift x values used in the vertical axis to facilitate the layering of all three spectra are 70, 0 and -60 for 3a, 4 and thiol spectra, respectively.

Part of the IR spectrum of polymer **4** is presented in Figure 1, sandwiched in between those of the two reagents used in the thiol-ene reaction: the polymeric allyl precursor **3a** (top) and the  $\text{CF}_3\text{-(CF}_2\text{)}_7\text{-(CH}_2\text{)}_2\text{-SH}$   $\text{C}_8$  thiol (bottom). As can be seen, the resulting spectrum for **4** is mostly a linear combination of the spectra for both reagents, with a higher weighing factor for the  $\text{C}_8$  thiol contribution. For example, the very intense bands of the difluoromethylene fragments (broad antisymmetric and symmetric stretching vibrations at 1195 and 1140  $\text{cm}^{-1}$ , respectively) fully hide the bands located in the same area and belonging to the original **3a** polymer. In areas where the added  $\text{CF}_3\text{-(CF}_2\text{)}_7\text{-(CH}_2\text{)}_2\text{-S}$  sulfide unit is not supposed to display any remarkable vibration bands, such as in the 1650-1790  $\text{cm}^{-1}$  region where C=O vibration are typically observed, the starting carbonyl stretch of **3a** at 1725  $\text{cm}^{-1}$  is maintained in **4** and clearly visible on its spectrum. In addition, the complete loss of the C=C stretching at 1645  $\text{cm}^{-1}$  and =CH<sub>2</sub> C-H antisymmetrical stretching at 3086  $\text{cm}^{-1}$  confirm the disappearance of the starting allyl groups and the efficiency of the thiol-ene reaction under the investigated conditions. As our initial objective had been to obtain a clean **4** devoid of significant structural defects, a very large excess of fluorinated thiol (10 equivalents) was used, ensuring an efficient capture of the generated free-radicals in the reaction chain involved in the mechanism.<sup>8</sup> As a result, no firm conclusion can be drawn yet regarding the efficiency of this “click” chemistry under economically viable conditions, i.e., with only a slight excess or no excess at all of the expensive thiol. Yet, it proved very valuable in yielding highly fluorinated **4** in a pure form and allowing for the in-depth characterization of its properties, as presented and discussed below.

**Thermal Properties of Fluorinated Polymer 4.** The thermal decomposition of **4** in air and under argon (used as an inert gas) was investigated by TGA (Figure 2). A first “low”-temperature decomposition that starts at 170-180°C in both cases and amounts to about 15% of

the initial mass is immediately followed by a second massive weight loss in the 250-400°C range. Based on the available literature, a share of the first decomposition can be assigned to the lateral  $\text{CF}_3\text{-(CF}_2)_7\text{-(CH}_2)_2\text{-S}$  sulfide unit. Similar low-temperature degradations to volatile products have indeed been described for a  $\text{CF}_3\text{-(CF}_2)_7\text{-(CH}_2)_2\text{-S}$ -modified silicone (starting decomposition at about 170°C) and a  $\text{CF}_3\text{-(CF}_2)_5\text{-(CH}_2)_2\text{-S}$ -modified oxazoline (starting decomposition at about 200°C).<sup>22-23</sup> In the second of the above studies, direct pyrolysis - mass spectrometry analysis of the involved thermal reactions unambiguously showed that the fluorinated thioether chains were responsible for the observed low-temperature decomposition. Yet, the decomposition is incomplete in this range of temperatures as a full degradation-volatilization of one  $\text{CF}_3\text{-(CF}_2)_7\text{-(CH}_2)_2\text{-S}$  would induce a weight loss of 44% (and 88% if both fluorinated units degrade to volatiles), in contrast to the observed 19% in Figure 2.

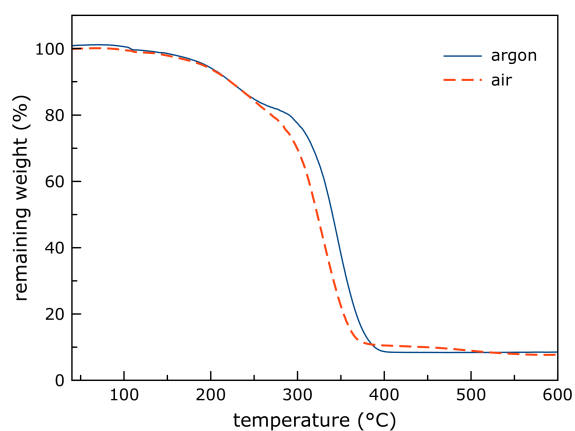


**Figure 2.** TGA thermogram of **4** in an argon (blue continuous line) or air atmosphere (red dashed line) at a heating rate of 10 K.min<sup>-1</sup>.

Heating **4** in the presence of oxygen did not influence the low-temperature decomposition, while the second degradation step – as expected - was faster, although not by a large factor (15 K shift in degradation temperature).

DSC curves corresponding to homopolymer **4** reveal two characteristic thermal transitions on heating: a low-temperature transition between 60 and 70°C and a high-temperature one between 90 and 115°C. The same two transitions are observed on cooling although with a significant hysteresis in their temperature positions (Figure 3).

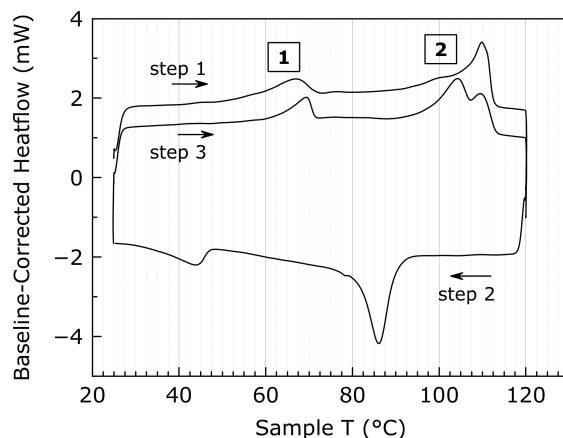
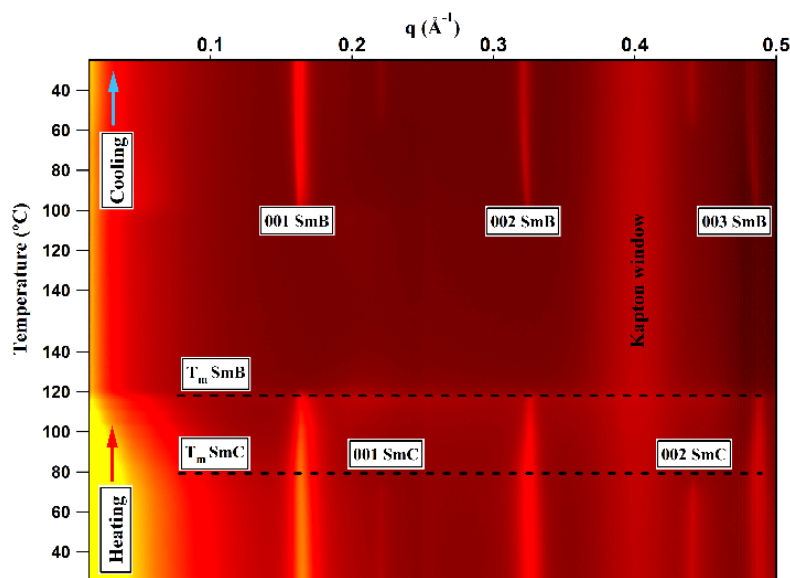


**Figure 3.** DSC thermogram for a sample of **4**: the three curves correspond to heating and cooling steps performed at a rate of 10 K.min<sup>-1</sup> in the order indicated in the figure.

**Solid-State Structure of Fluorinated Polymer 4.** Figure 4 shows the variable-temperature SAXS curves measured on **4** during a heating-cooling cycle. The heating and cooling ramps have been performed from room temperature to 140°C at a rate of 10 K.min<sup>-1</sup>. A short-term isotherm in the molten state preceded the cooling of the sample back to room temperature.

SAXS curves recorded at room temperature exhibit two sets of equidistant peaks in the q-space that can be ascribed to two different smectic phases. The smectic phase with the largest interlayer distance (38.5 Å) exhibiting much stronger peak intensities is tentatively ascribed to a SmB phase. The other smectic phase with a smaller interlayer distance (28.6 Å) can be identified as

SmC. In the latter case, it is expected that a bilayer of mesogens, i.e. the pendant fluorocarbon



chains, are inclined with respect to the normal to the smectic layers.

**Figure 4.** Variable-temperature SAXS data recorded on **4** during a heating-cooling cycle. The rate of temperature change was 10°C/min. The diffraction orders of the SmB and SmC phases are indicated.

The SmB and SmC phases reveal a difference in their thermal behavior. Thus, it can be seen that during heating the peaks pertinent to the SmC phase disappear at about 80°C leaving only the diffraction orders of the SmB phase. During further heating, the peaks of SmB persist up to ca. 120°C. Therefore, the minority SmC phase is found to be less thermodynamically stable than the dominant SmB phase, which could be accounted for by its higher specific surface. On cooling, the order of appearance of the phases is inverted, i.e., the peaks of the SmB phase show up first followed by those of the SmC phase.

In order to check the assignment of the dominant phase to SmB, additional experiments have been performed in grazing-incidence geometry (Figure 5). A thin film of **4** was formed on a Si

substrate from the melt, which cause the planes of the smectic layers to orient parallel to the substrate. This is indeed what one can observe on a room-temperature GIWAXS pattern on which the smectic diffraction orders are positioned on the meridional, or vertical, direction. Moreover, in addition to these peaks, a strong equatorial peak is observed at about 5 Å. This distance corresponds to packing of the PTFE-like chains, as previously noticed by Takahara *et al.*<sup>24</sup> It can be therefore concluded that the pendant fluorocarbon chains packed in a hexatic structure are standing upright in the film according to the structure of a SmB phase.

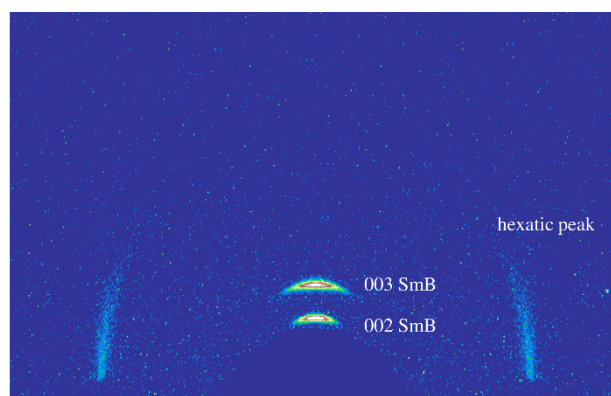


**Figure 5.** Room-temperature GIWAXS pattern of a thin film of **4** deposited from the melt. The diffraction orders of the dominant SmB phase are located on the meridional direction of the pattern, whereas the characteristic PTFE-like peak (hexatic peak) is positioned on the equator of the pattern.

Schematic illustration of the molecular organization in the SmB and SmC phases is shown in Figure 6. It can be seen that for the SmB phase the fluorocarbon mesogens displayed in the figure as light blue ellipsoids are oriented upright (Figure 6A) whereas they are inclined at an angle of ca. 46° in the SmC phase (Figure 6B). The details of the main-chain and pendant-chain

conformation for the two phases are given in panels C and D of the figure. It can be seen that despite the identical hexagonal packing of the pendant groups in the two phases, their disposition is different. Thus, if one looks along the direction of the main chain the fluorocarbons are stacked on top of each other for the SmB phase (Figure 6C) while they are disposed approximately in the same plane for the SmC phase (Figure 6C). The different configurations of the pendant groups described above become possible because the distance between carboxylic oxygens bonded to the same carbon is very close to that between the neighboring carboxylic oxygens in the direction along the main chain. Therefore, the mesogens can be equally well packed in rows running parallel and perpendicular to the main chain, which gives rise to the two co-existing liquid crystalline phases at room temperature. Such co-existence is quite unusual to thermotropic smectic phases formed by partially-ordered linear fluoroalkyl chains.<sup>25-27</sup>

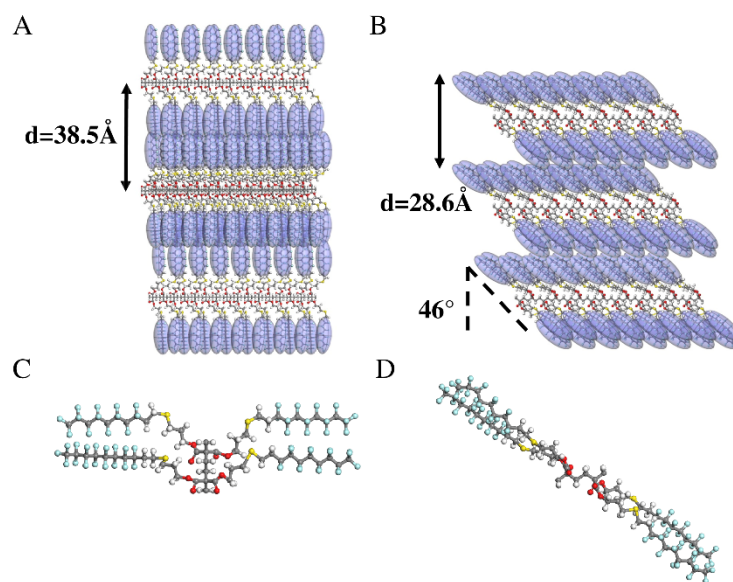


**Figure 6.** Schematics of the molecular arrangement in the SmB and SmC phases of **4**. The orientation and packing of the mesogens (light blue ellipsoids) for the SmB and SmC phases are

shown in A and B, respectively. The conformation of the main chain in the ball and stick representation is given in C and D.

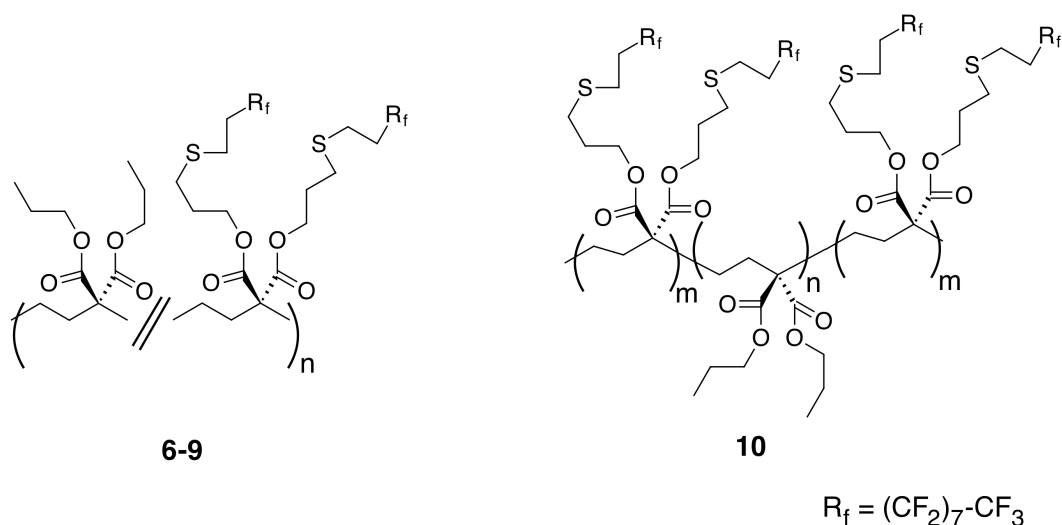
**Properties of the Shorter C<sub>6</sub>F<sub>13</sub>- Analog 5.** A polymer identical to **4** except for the size of the fluorinated chains (a C<sub>6</sub>F<sub>13</sub> rather than the C<sub>8</sub>F<sub>17</sub> used for **4**) could be obtained under the same thiol-ene conditions as the one described for **4** in Scheme 3 using the commercial C<sub>6</sub>F<sub>13</sub>-CH<sub>2</sub>CH<sub>2</sub>-SH thiol instead. The same basic properties (quantitative addition of the thiol to the polymer, polymer color and insolubility) as the ones described above for **4** could be observed (see Supplementary Information file for the FTIR and DSC data), except for its thermal behavior. DSC experiments indicated indeed that **5** does not display a simple behavior, with a major phase transition such as for **4** and copolymers of **4** (see next section). Instead, a very broad endotherm ranging 60 to 130°C could be observed (Figure S9), indicating most probably the much lower propensity of the shorter C<sub>6</sub>F<sub>13</sub> segment to self-organize.

Such a drastic difference between C<sub>8</sub>F<sub>17</sub>- and C<sub>6</sub>F<sub>13</sub>-substituted systems is not unprecedented. For example, in atactic polystyrenes displaying linear fluorinated chains of several sizes on the para-position of the lateral phenyl groups, a minimal size of eight carbons (C<sub>8</sub>F<sub>17</sub>) was required to induce side-chain crystallization, the C<sub>6</sub>F<sub>13</sub> system being entirely amorphous.<sup>28</sup> This is in agreement with a known tendency of alkyl chains in liquid crystalline molecules to improve the self-assembly process with the size of the chain. For example, for N-[3,4,5-tris-(alkyloxy)]benzoyl L-alanines whose supramolecular self-assembly was investigated using DSC and grazing-incidence X-ray diffraction analysis, an increase in alkyl length from 6 to 16 carbons induced a growing driving force for LC phase formation.<sup>27</sup> In addition, fluorinated linear chains are known to display a sharper increase in their self-assembling behavior with temperature than

their hydrogenated analogs. For example, to use an example pertinent to the above polymers, the difference in melting points between perfluorinated n-hexane and n-octane is 57 K while it is only 37 K for the corresponding n-alkanes. This trend was studied in greater details by Rabolt *et al.* for other fluorinated and partially fluorinated systems.<sup>29</sup>

This difference in the ability of **5** to self-assemble was further evidenced by SAXS (Figure S15). The one-dimensional scattering profile shows a single peak at  $0.017 \text{ \AA}^{-1}$  that indicates the formation of a poorly organized smectic phase with a lack of long-range order.

**Synthesis and Thermal Properties of Fluorinated Copolymers 6-10.** Copolymers containing both **4** repeat units – with  $\text{C}_8\text{F}_{17}$  side-chains – and di-*n*-propyl trimethylene-1,1-dicarboxylate units (i.e.,  $-\text{CH}_2-\text{CH}_2-\text{C}(\text{COOCH}_2-\text{CH}_2-\text{CH}_3)_2-$ ) – with *n*-propyl side chains – were also investigated. Statistical copolymers **6-9** with several compositions ranging from 20 to 80 mol-% in fluorinated units were synthesized from copolymers **3b-e** using the thiol-ene reaction of  $\text{C}_8\text{F}_{17}\text{C}_2\text{H}_4\text{SH}$  already described above for **3a** (see Scheme 3). Analogously, an ABA triblock copolymer **10** with a middle block B made of the propyl-substituted units and two external blocks A and C made of  $\text{C}_8\text{F}_{17}$ -substituted units was obtained from **3f**. The structures of **6-9** are available in Scheme 4.



**Scheme 4.** Structures of fluorinated copolymers **6-10**: **6-9** are statistical copolymers of the PolyC3 systems containing either fluorinated chains as in homopolymer **4** or n-propyl chains; **10** is a triblock copolymer containing two blocks analog to **4** separated by a PolyC3 block where the fluorinated chains are replaced by n-propyl groups

All copolymers, including **6** that contains only 20 mol-% in fluorinated units, were fully insoluble at room temperature as observed for homopolymer **4**. As expected, the IR spectra (available in the Supporting Information file, Figures S2 and S4-S8) display a massive non-linear increase in the  $(CF_2)$  signals with the fraction in fluorinated side-chains in the copolymers (see Figure S2). Several attempts were made to correlate quantitatively the absorbance of specific bands with the amounts in fluorinated chains, but unfortunately, no statistically validated relationships could be obtained. Interestingly, the width of the C=O vibration band at about  $1725\text{ cm}^{-1}$  was found to slightly spread with the increase in fluorinated chains. As for **4**, all vibration bands assignable to the starting allyl group had fully disappeared in copolymer spectra, suggesting that conversion had been complete in all case. The extremely large excess in starting thiol here again most probably plays a major role in the success of the reaction.

DSC thermograms for all copolymers are available in the Supplementary Information file (Figures S10-S14). The observed transitions are summarized in Table 2 along with the corresponding data for homopolymer **4**. A rather complex thermal behavior is observed for all systems, with typically low- and high-temperature transitions visible. The nature of the two main transitions for homopolymer **4** has been identified based on variable-temperature SAXS and GIWAXS experiments (see above text). Importantly, the main, i.e., high-temperature, endotherm for **4** displays a clearly composite character, containing two and more components.

**Table 2.** Influence of the architecture on the melting temperature of polymers **4** and **6-10** that all contain repeat units with C<sub>8</sub>F<sub>17</sub> lateral chains (see Schemes 3 and 4 for the corresponding drawn structures).

	Polymer Architecture	M <sub>n</sub> of precursor <b>3a-3f</b> <sup>a</sup> (× 10 <sup>-3</sup> )	M <sub>w</sub> /M <sub>n</sub> of precursor <b>3a-3f</b> <sup>a</sup>	Fraction of fluorinated units in the polymers (mol-%)	Transition <sup>b</sup>	
					temperature(s) (°C)	endotherm (J.g <sup>-1</sup> )
<b>6</b>	statistical copolymer	12.0	1.17	20	72 (main)	31.4
					28 (minor)	< 0.2
<b>7</b>	statistical copolymer	11.0	1.23	40	79 (minor)	0.6
					87 (main)	18.3
<b>8</b>	statistical copolymer	4.0	1.09	60	77	27.4
					- 6	5.1
<b>9</b>	statistical copolymer	4.6	1.13	80	80	25.4
					- 8	2.9
<b>4</b>	homopolymer	9.2	1.21	100	74	2.1

					109	10.0
<b>10</b>	triblock copolymer	9.3	1.10	40	76	33.3

<sup>a</sup> SEC-MALLS; <sup>b</sup> as obtained by DSC measurements (-50 to 150°C scanning range, heating rate = 10 K.min<sup>-1</sup>, followed by a cooling step back to -50°C at 40 K.min<sup>-1</sup>, and a second heating at 10 K.min<sup>-1</sup>, reported data points refer to the second heating step and the onset temperatures).

The details of the high-temperature peak shape vary as a function of the sample thermal history, which prompts us to identify this phenomenon with the well-documented crystalline or LC phase reorganization typical of comb-like polymers with flexible side groups.<sup>30-32</sup> In this case, the structure reveals a pronounced tendency to anneal (perfect) while heated in a DSC operated at moderate heating rates, and show the peaks that reflect such a process.<sup>33</sup> It is noteworthy that the SAXS curves display variable peak width as a function of annealing conditions (not shown here), although without any major change in the structure. Therefore, the structural perfection operates indeed during the DSC ramps and can account for the occurrence of complex melting patterns.

For statistical copolymers **6-9** (Table 2, entries 1-4), an even more complicated pattern could be observed, probably as the result of the increased difficulty for the fluorinated chains to self-assemble when further diluted in the polymer matrix. In all cases, the high-temperature peak typical of the homopolymer **4** disappeared, while the low-temperature peak remained in place in the 72-80°C range. Further peaks at lower temperatures could also be observed. As these systems are clearly far away from thermodynamic equilibrium, it can be expected that the appearance of these peaks also strongly reflect the kinetics required for the fluorinated chains to move and find each other during the self-assembling process, and that extended annealing could strongly impact

the thermograms. A more detailed investigation would be interesting, but has not been performed yet.

For the ABA triblock copolymer **10** where two blocks identical to homopolymer **4** are separated by a PolyC<sub>3</sub> block containing n-propyl branches and no fluorinated chains, only the low-temperature peak could be identified, suggesting that the central block makes the molecular organization discussed above for **4** more difficult to achieve due to a mismatch between the structural requirements imposed by the two blocks.

## CONCLUSIONS

Homopolymers and copolymers containing  $-\text{CH}_2-\text{CH}_2-\text{C}(\text{COOR})_2-$  subunits, with R displaying a long fluorinated carbon chain, can be cleanly obtained by the thiol-ene reaction of fluorinated thiols on polymer precursors of the same type where the R group is an allyl. Despite the fact the obtained homopolymers have a very high density of pendent fluorinated chains, full modification can be obtained when using a high molar excess of thiol.

All obtained polymers are poorly soluble in organic solvents, including fluorinated ones at room temperature. The displayed solubility is much lower than those reported in the literature for polymers containing identical or similar lateral perfluorinated carbon chains.

The phase behavior of the C<sub>8</sub>F<sub>17</sub> homopolymer was addressed using variable-temperature SAXS and GIWAXS techniques. They consistently show a coexistence of two smectic phases at room temperature, which can be identified as SmB and SmC. The reason for such coexistence is attributed to the fact that the distances between carboxylic oxygens bonded to the same carbon are very close to the ones between the neighboring carboxylic oxygens alongside the backbone. This results in the formation of two independent conformers with different packing modes for the pendant fluoroalkyl chains arranged in an hexatic order. The resulting structure is characterized

by a marked capacity to anneal (reorganize), in close similarity with the multiple-melting behavior documented for semicrystalline polymers.

## **ASSOCIATED CONTENT**

### **Supporting Information**

The following file is available free of charge on the ACS Publication website: fluoroPolyC3 (si).pdf (2000-4000  $\text{cm}^{-1}$  extension of the limited IR spectrum displayed in Figure 1, overlapping of the FTIR spectra for copolymers **6-9**, and the full IR spectra and DSC thermograms for polymers **5-10**).

## **AUTHOR INFORMATION**

### **Corresponding Authors**

\*Dimitri A. Ivanov: Phone 33 (0)3 89608807 E-mail: Dimitri.ivanov@uha.fr;

\* Jacques Penelle: Phone 33 (0)1 49781275 E-mail: penelle@icmpe.cnrs.fr

### **Author Contributions**

The manuscript was written through contributions of all authors. All authors have given approval to the final version of the manuscript.

## **ACKNOWLEDGMENTS**

We are very indebted to Valessa Barbier who supervised some of the early experiments presented in this contribution, as well as to Tina Modjinou for the CP/MAS NMR experiment. The authors acknowledge the Ministry of Science and High Education of the Russian Federation

(contract No. 14.587.21.0052 (RFMEFI58718X0052)), the East-Paris University and the CNRS for financial support, as well as the French Ministry for Foreign Affairs for travel funding via the Kolmogorov program (Innovative Materials for Advanced Purification and Metal recovery Processes). The authors are grateful to D. Hermida-Merino (ESRF) for excellent technical support during synchrotron experiments at the BM26B beamline.

## REFERENCES

1. Gardiner, J. Fluoropolymers: Origin, Production, and Industrial and Commercial Applications. *Aust. J. Chem.* **2015**, *68*, 13-22.
2. Améduri, B. Fluoropolymers: The Right Material for the Right Applications. *Chem. Eur. J.* **2018**, *24*, 18830-18841.
3. Nyuui, T.; Matsuba, G.; Sato, S.; Nagai, K.; Fujimori, A. Correlation between Gas Transport Properties and the Morphology/Dynamics of Crystalline Fluorinated Copolymer Membranes. *J. Appl. Polym. Sci.* **2018**, *135*, 45665/1-45665/9.
4. Knight, J. C.; Edwards, P. G.; Paisey, S. J. Fluorinated Contrast Agents for Magnetic Resonance Imaging. A Review of Recent Developments. *RSC Adv.* **2011**, *1*, 1415-1425.
5. Shimomoto, H.; Kudo, T.; Tsunematsu, S.; Itoh, T.; Ihara, E. Fluorinated Poly(substituted methylene)s Prepared by Pd-Initiated Polymerization of Fluorine-Containing Alkyl and Phenyl Diazoacetates: Their Unique Solubility and Postpolymerization Modification. *Macromolecules* **2018**, *51*, 328-335.
6. Illy, N.; Boileau, S.; Winnik, M. A.; Penelle, J.; Barbier, V. Thiol-Ene "Clickable" Carbon-Chain Polymers Based on Diallyl Cyclopropane-1,1-Dicarboxylate. *Polymer* **2012**, *53*, 903-912.
7. Morcombe, C. R.; Zilm, K. W. Chemical Shift Referencing in MAS Solid State NMR. *J. Magn. Reson.* **2003**, *162*, 479-486.
8. Lowe, A. B. Thiol-Ene "Click" Reactions and Recent Applications in Polymer and Materials Synthesis: A First Update. *Polym. Chem.* **2014**, *5*, 4820-4870.

9. Fiore, M.; Berth, N.; Renaudet, O.; Barbier, V. New Glycopolymers as Multivalent Systems for Lectin Recognition. *MedChemComm* **2014**, *5*, 1202-1207.
10. Illy, N.; Majonis, D.; Herrera, I.; Ornatsky, O.; Winnik, M. A. Metal-Chelating Polymers by Anionic Ring-Opening Polymerization and Their Use in Quantitative Mass Cytometry. *Biomacromolecules* **2012**, *13*, 2359-2369.
11. Shimizu, T.; Tanaka, Y.; Kutsumizu, S.; Yano, S. Ordered Structure of Poly(1H,1H-fluoroalkyl  $\alpha$ -fluoroacrylate)s. *Macromolecules* **1996**, *29*, 156-164.
12. Corpart, J. M.; Girault, S.; Juhue, D. Structure and Surface Properties of Liquid Crystalline Fluoroalkyl Polyacrylates: Role of the Spacer. *Langmuir* **2001**, *17*, 7237-7244.
13. Pees, B.; Sindt, M.; Paul, J. M.; Mieloszynski, J. L. Synthesis and Physico-Chemical Characterization of  $\omega$ -Perfluorooctyl-alkyl Polyacrylates: Odd-Even Effect. *Eur. Polym. J.* **2002**, *38*, 921-931.
14. Shimomoto, H.; Fukami, D.; Kanaoka, S.; Aoshima, S. Fluorinated Vinyl Ether Homopolymers and Copolymers: Living Cationic Polymerization and Temperature-Induced Solubility Transitions in Various Organic Solvents Including Perfluoro Solvents. *J. Polym. Sci. Pol. Chem.* **2011**, *49*, 2051-2058.
15. Shimomoto, H.; Fukami, D.; Kanaoka, S.; Aoshima, S. Fluorine-Containing Vinyl Ether Polymers: Living Cationic Polymerization in Fluorinated Solvents as New Media and Unique Solubility Characteristics in Organic Solvents. *J. Polym. Sci. Pol. Chem.* **2011**, *49*, 1174-1182.

16. Gress, A.; Völkel, A.; Schlaad, H. Thio-Click Modification of Poly[2-(3-butenyl)-2-oxazoline]. *Macromolecules* **2007**, *40*, 7928-7933.
17. Yin, Q.; Alcouffe, P.; Beyou, E.; Charlot, A.; Portinha, D. Controlled Perfluorination of Poly(2,3,4,5,6-pentafluorostyrene) (PPFS) and PPFS-Functionalized Fumed Silica by Thiol-Para-Fluoro Coupling: Towards the Design of Self-Cleaning (Nano)Composite Films. *Eur. Polym. J.* **2018**, *102*, 120-129.
18. Schwarz, R.; Seelig, J.; Künnecke, B. Structural Properties of Perfluorinated Linear Alkanes: A  $^{19}\text{F}$  and  $^{13}\text{C}$  NMR Study of Perfluorononane. *Magn. Reson. Chem.* **2004**, *42*, 512-517.
19. Foris, A.  $^{13}\text{C}$  NMR Spectra of Halocarbons. *Magn. Reson. Chem.* **2001**, *39*, 386-398.
20. Pretsch, E.; Seibl, J.; Simon, W.; Clerc, T., *Tables of Spectral Data for Structure Determination of Organic Compounds*. Springer-Verlag: Berlin, 1983.
21. Breitmaier, E.; Voelter, W., *Carbon-13 NMR Spectroscopy*. VCH: Weinheim, 1987.
22. Hayase, G.; Kanamori, K.; Hasegawa, G.; Maeno, A.; Kaji, H.; Nakanishi, K. A Superamphiphobic Macroporous Silicone Monolith with Marshmallow-Like Flexibility. *Angew. Chem. Int. Ed.* **2013**, *52*, 10788-10791.
23. Atilkan, N.; Schlaad, H.; Nur, Y.; Hacaloglu, J. Direct Pyrolysis - Mass Spectrometry Analysis of Thermal Degradation of Thio-Click-Modified Poly(2-oxazoline). *Macromol. Chem. Phys.* **2014**, *215*, 148-152.
24. Ishige, R.; Shinohara, T.; White, K. L.; Meskini, A.; Raihane, M.; Takahara, A.; Améduri, B. Unique Difference in Transition Temperature of Two Similar Fluorinated Side Chain Polymers Forming Hexatic Smectic Phase: Poly{2-(perfluorooctyl)ethyl

- acrylate} and Poly(2-(perfluorooctyl)ethyl vinyl ether). *Macromolecules* **2014**, *47*, 3860–3870.
25. Zhu, X.; Mourran, A.; Beginn, U.; Moeller, M.; Anokhin, D. V.; Ivanov, D. A. Self-Assembled Structures Formed by a Wedge-Shaped Molecule in 2D and 3D: The Role of Flexible Side Chains and Polar Head Groups. *Phys. Chem. Chem. Phys.* **2010**, *12*, 1444-1452.
26. Anokhin, D. V.; Defaux, M.; Mourran, A.; Moeller, M.; Luponosov, Y. N.; Borshchev, O. V.; Bakirov, A. V.; Shcherbina, M. A.; Chvalun, S. N.; Meyer-Friedrichsen, T.; Elschner, A.; Kirchmeyer, S.; Ponomarenko, S. A.; Ivanov, D. A. Effect of Molecular Structure of  $\alpha,\alpha'$ -Dialkylquaterthiophenes and Their Organosilicon Multipods on Ordering, Phase Behavior, and Charge Carrier Mobility. *J. Phys. Chem. C* **2012**, *116*, 22727-22736.
27. Anokhin, D. V.; Lejnieks, J.; Mourran, A.; Zhu, X.; Keul, H.; Moeller, M.; Konovalov, O.; Erina, N.; Ivanov, D. A. Interplay between H-Bonding and Alkyl-Chain Ordering in Self-Assembly of Monodendritic L-Alanine Derivatives. *ChemPhysChem* **2012**, *13*, 1470-1478.
28. Bouteiller, V.; Garnault, A.M.; Teyssié, D.; Boileau, S.; Möller, M. Synthesis, Thermal and Surface Characterization of Fluorinated Polystyrenes. *Polym. Int.* **1999**, *48*, 765-772.
29. Rabolt, J.F.; Russell, T.P.; Twieg, R.J. Structural Studies of Semifluorinated n-Alkanes. 1. Synthesis and Characterization of  $F(CF_2)_n(CH_2)_mH$  in the Solid State. *Macromolecules* **1984**, *17*, 2786-2794.

30. Shi, H.; Zhao, Y.; Dong, X.; Zhou, Y.; Wang, D. Frustrated Crystallisation and Hierarchical Self-Assembly Behaviour of Comb-Like Polymers. *Chem. Soc. Rev.* **2013**, *42*, 2075–2099.
31. Danke, V.; Gupta, G.; Huth, H.; Schawe, J.; Beiner, M. Polymorphic States and Phase Transitions in a Comb-Like Polymer Having a Rigid Polyester Backbone and Flexible Side Chains. *Thermochim. Acta* **2019**, *667*, 162-168.
32. Gupta, G.; Danke, V.; Babur, O.; Beiner, M. Interrelations Between Side Chain and Main Chain Packing in Different Crystal Modifications of Alkoxylated Polyesters. *J. Phys. Chem. B* **2017**, *121*, 4583-4591.
33. Melnikov, A. P.; Rosenthal, M.; Ivanov, D. A. Thermal Analysis of Semicrystalline Polymers: Exploring the General Validity of the Technique. *ACS Macro Lett.* **2018**, *7*, 1426–1431.